

Possibility of Protection Against UWB Pulses Based on a Turn of a Meander Microstrip Line

Roman Sergeevich Surovtsev, Alexander Vyacheslavovich Nosov, Alexander Mikhailovich Zabolotsky, and Talgat Rashitovich Gazizov

Abstract—Decomposition of an ultrawideband (UWB) pulse into a sequence of pulses with lower amplitudes in a turn of a meander microstrip line has been experimentally proved to be an effective method of protection against UWB pulses for electronic equipment. It has been shown that the output signal of the line can be minimized by means of equalization of amplitudes of the first three pulses. It has been achieved due to optimization of coupling between half-turns of the line. The obtained attenuation of a pulse with full-width-at-half-maximum of 40 ps is 6.3 times. Combination of experimental and simulation methods is used to obtain the results in time and frequency domains.

Index Terms—Delay lines, protection, time domain analysis.

I. INTRODUCTION

NOWADAYS, to ensure reliable operation of communication systems, it is urgent to protect electronic devices from intentional electromagnetic interference (IEMI) of nanosecond and subnanosecond pulses. Such ultrawideband (UWB) pulses are able to penetrate into electronic equipment bypassing electromagnetic shields and can cause malfunction of electric circuits. For example, a group of Chechen fighters used a UWB pulses generator to block the radio communication of Russian troops; in 2012, one of the largest British banks was blackmailed by terrorists who threatened to break the security system and bank computers via high power electromagnetic pulses [1]. The above-mentioned examples are just a few of many other disclosures, and their number has been increasing lately. Therefore, a number of outstanding projects such as Protection of Critical Infrastructures against High Power Microwave Threats, Strategies for The impROvement of critical infrastrUCTure Resilience to Electromagnetic attackS, and SEcURITY of Railways against Electromagnetic aTTacks are aimed at protection of strategically important infrastructure (power stations, railways, communication systems, computer networks, etc.) against IEMI.

Traditional protection devices do not protect properly from strong UWB pulses [2]. Thus, new methods of protection should

be developed and new protection devices should be created. Meander lines are used for filtration of a signal in a frequency band [3], all-pass characteristics of a meander line turn are presented in the classic paper [4]. The electronic equipment can be protected against UWB pulses by means of meander lines as in such case we do not have to add additional components to a printed circuit, and we can also use traditional elements of a printed circuit board, i.e., meander delay lines [5]–[8]. In comparison to existing widely used protective devices, this approach does not require additional components and devices integrated into the printed circuit, and allows usage of traditional protective elements of printed circuits – meander delay lines. Meander lines are radiation resistant and can work for a very long time since they do not contain either semiconductor (in contrast to various filters) or degrading elements (in comparison to the lightning arrester with a limited number of operations). Besides, meander lines in contrast to components lack the parasitic inductance of the leads, and it is inexpensive to design the meander lines and use them. These advantages of meander lines against traditional protective devices prove the urgency of the research dedicated to the implementation of meander lines for the protection against UWB pulses. Sometimes UWB pulses can penetrate into the equipment bypassing electromagnetic shields. The pulses produce electromagnetic field inside the equipment and introduce interference at all lines of the equipment. In such cases, the protective method described above can be used outside the equipment in the form of an intermediate structure between the equipment and outside cables in order to exclude the influence of UWB pulses.

The common disadvantage of investigations of meander lines described in [5]–[8] is that they are based on simulation only, moreover, simulation of perfect structures, but not the simulation of interconnections of real circuit boards, in which losses and dispersion may have significant influence on the results. Another disadvantage is that only perfect excitations are used during simulation, but not real ones. Thus, if we want to prove that it is possible to decompose a UWB pulse in the turn of a meander line and that it is possible to minimize the amplitude of a UWB pulse by means of the equalization of amplitudes of the first three pulses, then it is essential to carry out simulation with a real excitation and consider losses in conductors and dielectrics as well as to compare the results with results of a full-scale experiment.

The aim of this paper is to prove experimentally that distortions in the turn of a meander microstrip line can be used to

Manuscript received May 11, 2016; revised October 6, 2016 and January 31, 2017; accepted March 1, 2017. Date of publication March 22, 2017; date of current version August 17, 2017. This work was supported as follows: Mathematical modeling was supported by the state contract 8.9562.2017/BP of the Russian Ministry of Education and Science. Simulation was supported by the Russian Foundation for Basic Research under Grant 14-29-0925. Experiment was supported by the Russian Science Foundation under Grant 14-19-01232 in the Tomsk State University of Control Systems and Radioelectronics.

The authors are with the Tomsk State University of Control Systems and Radioelectronics, Tomsk 634050, Russia (e-mail: surovtsvrs@gmail.com; alexns94@gmail.com; zabolotsky_am@mail.ru; talgat@tu.tusur.ru).

Digital Object Identifier 10.1109/TEMC.2017.2678019

protect electronic equipment against UWB pulses. It requires optimization of the cross section of the line in order to minimize reflections in the measuring channel that occur during a full-scale experiment. It is necessary to produce a printed circuit with a set of models of meander lines and to evaluate deviations of real parameters' values from their preliminary optimization values. The next step is a full-scale experiment and, finally, the comparison of results of the experiment with results of the simulation of waveforms at the end of a meander line turn.

II. BACKGROUND

A series of experiments has already been carried out to demonstrate the possibility of protection against UWB pulses by means of the meander line [5]–[8]. Let us briefly describe these research results.

The physical principle of the proposed protection is based on the phenomenon of the UWB pulse decomposition into a sequence of pulses with lower amplitudes which is achieved by means of the optimal choice of parameters of the line. For the first time, this method was investigated on the example of a turn of an asymmetrical meander line in the air [5]. Detailed analysis of pulse distortions proved that it was possible to decrease the amplitude of a UWB pulse by means of its decomposition into two pulses (crosstalk and the basic signal) of lower amplitudes. To do the above described we should provide some conditions.

First of all, the influence of the near-end crosstalk on a waveform shall be excluded; delay in a line shall be longer than the sum of the front (t_r), flat top (t_d), and fall (t_f) of the pulse signal [9]

$$2 \cdot \tau \cdot l \geq t_r + t_d + t_f \quad (1)$$

where l is length of a half-turn, $\tau = \tau_e = \tau_o$ [per-unit-length delays of even (τ_e) and odd (τ_o) modes of a signal are always equal if it is propagating in a homogeneous dielectric].

Second, the edge coupling between conductors of a line shall be strong, as its optimization helps to minimize the amplitude of the output signal because pulse amplitudes of the crosstalk and a basic signal become closer. During the investigation, the maximum attenuation of a UWB pulse was 1.6 times.

Fig. 1 clearly shows changes in waveforms that occur as the above-mentioned conditions are fulfilled. The figure shows UWB pulses at the input and output of a meander line when the first and the second conditions are fulfilled. The duration of the input UWB pulse [see Fig. 1(a)] equals to $2 \cdot \tau \cdot l$ in order to meet the condition (1). We can see from Fig. 1(b) that if the condition (1) is fulfilled, the pulse of the main signal comes after the near end crosstalk, and the crosstalk does not influence the main signal. The stronger edge coupling between conductors obtained by means of the optimal separation of conductors leads to the equalization of amplitudes of the first and the second pulses of a signal (the amplitude of the first pulse is increased, the amplitude of the second pulse is decreased) at the output of the line [see Fig. 1(c)]. To decompose and equalize pulses, both the first and the second conditions should be under control, as optimization of the gap between signal conductors leads to changes in the per-unit-length delay. It may lead to the overlap of the crosstalk

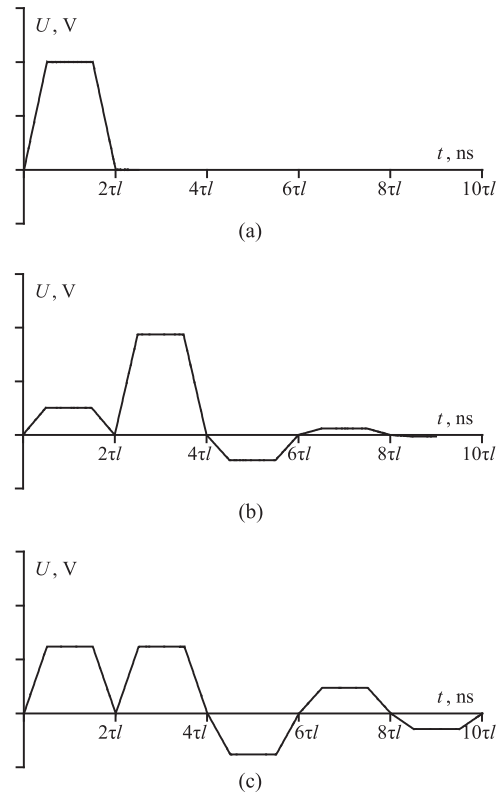


Fig. 1. Waveforms of UWB pulses at the input (a) and output of a meander line with the first (b) and the second (c) conditions fulfilled.

and the main signal; thus, the amplitude of the output signal may be increased.

Similar analysis of a meander line turn of a microstrip line was carried out in [6]. As long as a microstrip has an inhomogeneous dielectric filling, τ_e does not equal τ_o . Therefore, to exclude the near end crosstalk, one should rewrite (1) as

$$2 \cdot \tau_{\min} \cdot l \geq t_r + t_d + t_f \quad (2)$$

where τ_{\min} – the minimum value of per-unit-length delays of even and odd modes of the line.

It has been revealed in [5] that one should additionally decompose the basic signal into pulses of even and odd modes in order to minimize amplitudes of the result of the UWB pulse decomposition. The condition is

$$2 \cdot |\tau_e - \tau_o| \cdot l \geq t_r + t_d + t_f. \quad (3)$$

The UWB pulse at the end of the line will be decomposed into three pulses (crosstalk pulse and pulses of even and odd modes) and, if the coupling between the conductors is optimal, their amplitudes will be minimal and equal. The maximum attenuation of the UWB pulse amplitude was 2.5 times during the investigation.

We extended the described research by the simulation of the meander line with a broadside coupling. This simulation accounts for losses in conductors and dielectrics as there are losses in interconnections of real printed circuits. These losses significantly influence distortion of the output signal [8]. The simulation has proved that if we take into account losses, the

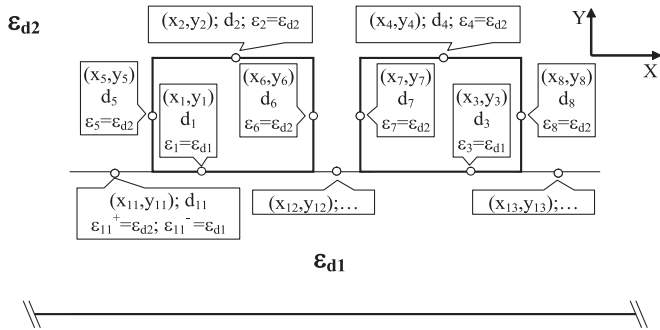


Fig. 2. Segmentation of cross section boundaries.

UWB pulse amplitude can be additionally attenuated. The paper also states that due to losses, in addition to the attenuation of the UWB pulse amplitude, the optimal value of the gap between conductors increases which is advantageous for the practical implementation of meander lines.

III. PRELIMINARY SIMULATION AND PREPARATION OF EXPERIMENT

Before the simulation and full-scale experiment can be performed, we should carry out preliminary optimization of parameters of the cross section of the line [10]. In order to minimize reflections in the measuring circuit, the geometric mean of the characteristic impedance of even (Z_e) and odd (Z_o) modes of the line is set to be 50Ω . Below we describe in detail the method for computation of matrix parameters and give the results of the optimization of the meander line turn for the experiment.

A. Research Methods

As long as the meander line turn is a coupled short-circuit transmission line, any traditional approach to the transmission line simulation can be used for the simulation of the signal propagation in a turn of a meander line. Before that we should compute matrixes of per-unit-length coefficients of electromagnetic and electrostatic inductions of the line segment (matrixes \mathbf{L} and \mathbf{C}). Quasistatic approach based on the method of moments is the simplest and the most effective method of calculation. Fig. 2 shows the cross section of coupled lines with an infinite ground plane. First, we need to carry out the segmentation (separation into elementary segments – subintervals) of structure boundaries.

Every n th subinterval can be described by the following parameters: x_n – X-coordinate of the center of subinterval n ; y_n – Y-coordinate of the center of subinterval n ; d_n – length of subinterval n ; ε_n – dielectric permittivity near the n th subinterval conductor-dielectric; and ε_n^+ and ε_n^- – dielectric permittivities at the positive and negative sides of the n th subinterval dielectric-dielectric relatively to X or Y axis. These parameters are used to compute elements of the square and dense matrix \mathbf{S} . Solution of linear systems with matrix \mathbf{S} for every N_{COND} right-side vectors (based on the total number of signal conductors in the structure) gives the distribution of the charge at boundaries of the structure, from which coefficients of the matrix \mathbf{C} are calculated. Matrix \mathbf{L} can be calculated as a product of the dielectric

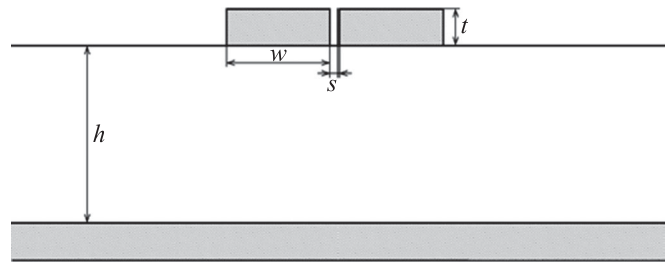


Fig. 3. Cross section of the meander microstrip line.



Fig. 4. Circuit diagram of the meander microstrip line.

permittivity of the vacuum ε_0 , magnetic permeability of the vacuum μ_0 , and matrix that is inverse to the matrix \mathbf{C} computed using the same approach but with the relative dielectric permittivity of every dielectric equal to the inverse value of its relative magnetic permeability. Paper [11] describes in details models for computation of matrices \mathbf{L} and \mathbf{C} . Losses are taken into account in a more detailed simulation. In addition to matrices \mathbf{L} and \mathbf{C} , matrices of per-unit-length conductance \mathbf{G} (losses in dielectric) and resistance \mathbf{R} (losses in conductors) are computed. Then we construct an equivalent scheme of the line, assign all matrices of per-unit-length parameters to it, and define the length of the line as well as the input excitation in time domain. Response to the excitation is computed in frequency domain using the modified node potential method based on solution of telegraph equations and the time response is obtained by means of the inverse fast Fourier transformation. The described simulations were carried out in the TALGAT software which allows solution of a wide range of electromagnetic compatibility problems [12] and is used for simulations represented in this paper.

B. Optimization of Parameters of the Line Cross Section

A standard material, foiled fiberglass FR-4 without protecting soldering mask, was chosen as a material for the printed circuit board. Thickness of the core for the printed circuit is $h_C = 2000 \mu\text{m}$, thickness of the foil is $t = 35 \mu\text{m}$, the dielectric permittivity of the substrate is 5.4. Cross section of every model of the meander line corresponds to a coupled microstrip line without coverings (see Fig. 3). As some parameters of the cross section of the line have typical values, only two parameters were optimized – the width of the signal conductor w and the gap between signal conductors s . After the optimization, we determined the width of the conductor as $w = 2500 \mu\text{m}$, the gap between conductors of the first model as $s = 250 \mu\text{m}$. For all following models, the gap was being successively reduced down to $100 \mu\text{m}$ in increments of $50 \mu\text{m}$ in order to strengthen the coupling between signal conductors and to evaluate the possibility of equalization of amplitudes of the first three pulses.

Fig. 4 shows the schematic of connections of the line from Fig. 1 consisting of two parallel conductors with the length l interconnected at one end. One of the conductors is connected

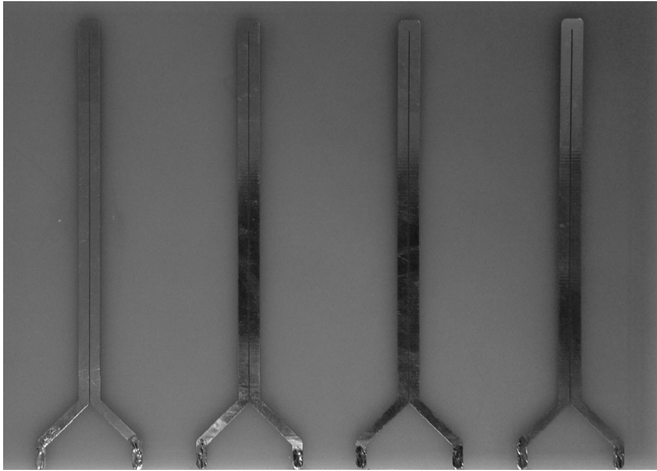


Fig. 5. Printed circuit board with models of meander delay lines.

to a pulse source, which is presented by the electromotive force source E and the internal resistance $R1$. Another conductor is connected to a receiving unit, which is shown as $R2$. During the simulation, $R1$ and $R2$ are equal to 50Ω .

Next, we should choose l that fulfills the condition (3) for the decomposition of a UWB pulse into pulses of even and odd modes. Since the full-scale experiment will be carried out by means of an oscilloscope C9-11 (50Ω internal impedance, 17.8 GHz bandwidth), the duration of a pulse provided by generator is known to equal to about 100 ps. Using (3) we can compute the minimum length of the half-turn of the line l which is necessary for the decomposition of a UWB pulse into a sequence of pulses. Values of $\tau_e = 6.63 \text{ ns/m}$ and $\tau_o = 5.80 \text{ ns/m}$ are calculated by the method of moments for the half-turn with $s = 250 \mu\text{m}$ and used to calculate l . The minimum l that fulfills the condition (3) is 60.3 mm. As the full-scale experiment is being carried out with real UWB pulses and a real printed circuit, we should take into account that the UWB pulse in the real interconnection may be incompletely decomposed into pulses of even and odd modes because of dispersion, losses, and some other factors. Note that amplitudes of pulses in the output of the line are greatly dependent on the duration of UWB pulses as the increase of the signal front (which is typical for real interconnections) is stronger for a shorter duration than for a longer one. To exclude the factors described above, l was set to 90 mm.

Using the results of the preliminary optimization, a printed circuit board with models of meander delay lines has been produced from the two-sided fiberglass FR-4 (see Fig. 5). The length of each half-turn is 90 mm, connections are $(2w + s)$.

After the circuit board had been manufactured, we used a measuring magnifier in form of a loupe with a ruler (division value 0.1 mm) and a micrometer (division value 0.01 mm) to measure its real geometric parameters: $w = 2450 \mu\text{m}$, $s = 300, 250, 200, 150 \mu\text{m}$, $t = 45 \mu\text{m}$, $h_C = 2000 \mu\text{m}$. According to the measured data, we computed τ_e and τ_o , $\Delta\tau = \tau_e - \tau_o$, Z_e , Z_o , $\sqrt{(Z_e Z_o)}$ which are given in Table I.

It is clear from Table I that the per-unit-length delay of even mode is unchanged for all models of meander lines, and the per-unit-length delay of odd mode is decreasing simultaneously

TABLE I
PARAMETERS OF THE MANUFACTURED MODELS OF MEANDER DELAY LINES

$s, \mu\text{m}$	$\tau_e, \text{ns/m}$	$\tau_o, \text{ns/m}$	$\Delta\tau, \text{ns/m}$	Z_e, Ω	Z_o, Ω	$\sqrt{(Z_e Z_o)}, \Omega$
300	6.720	5.944	0.776	33.636	72.974	49.544
250	6.719	5.922	0.797	32.342	73.384	48.717
200	6.719	5.894	0.824	30.820	72.805	47.694
150	6.718	5.853	0.865	28.953	74.237	46.362

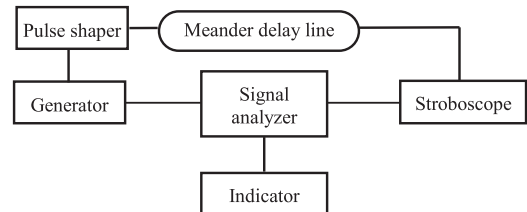


Fig. 6. Schematic figure of the experimental setup.

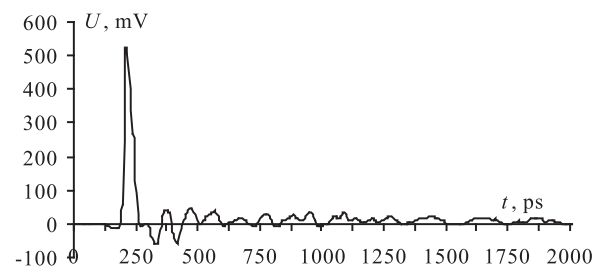


Fig. 7. Oscilloscope record of a signal at the output of the generator.

with s which causes increase of $\Delta\tau$. It is also worth noting that the decrease of s leads to a slight (down to 3Ω) decrease of $\sqrt{(Z_e Z_o)}$ which may cause changes of pulse amplitudes in the full-scale experiment.

C. Experimental Setup

The experimental setup was based on the stroboscopic oscilloscope C9-11 comprising of the signal analyzer, indicator, generator, stroboscope. and pulse shaper (see Fig. 6). A 20 dB attenuator was connected to the stroboscope input to protect it. The meander delay line was connected to the pulse shaper and the attenuator through sub-miniature version A (SMA) connectors.

Each experiment has been performed in the following order. First, the UWB pulse from the pulse shaper propagated to the input connector, then directly (without meander delay line) to the output connector and, at last, to the attenuator and the stroboscope input to measure the signal waveform. Afterward, the meander delay line was connected between the input and output connectors and the resulting signal waveform was measured.

IV. RESULTS OF EXPERIMENT AND SIMULATION

A. Results of the Experiment

During the experiment, a signal of 40 ps at half of the maximum level (527 mV) was supplied from the output of the generator to the input of the combined oscilloscope C9-11. Fig. 7

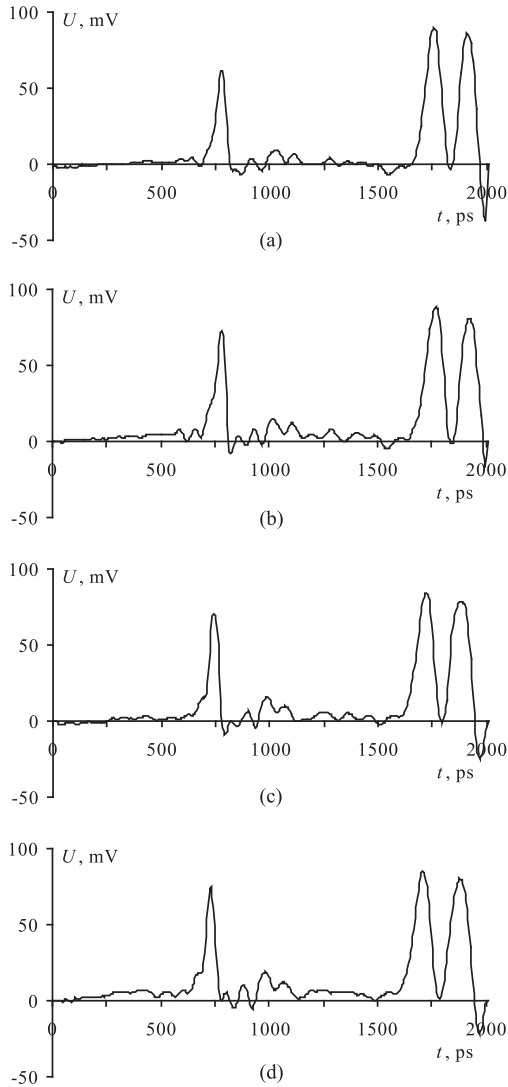


Fig. 8. Oscilloscope records of the signal at the output of models of meander lines for $s = 300$ (a), 250 (b), 200 (c), 150 (d) μm .

shows an oscilloscope record of a signal at the output of the generator.

Models of the lines were successively inserted between the output of the generator and the input of the oscilloscope. Fig. 8 shows the oscilloscope records of a signal at the output of each model. Oscilloscope records show that the signal at the end of all lines is a sequence of three basic pulses, where the first pulse is a crosstalk at the near end, the second and the third are pulses of even and odd modes. Obtained oscilloscope records contain the results we have expected. To obtain numerical coincidence of the experiment and simulation results, we will use the real excitation (for example, by means of the digitization of an oscilloscope record of a signal at the output of the generator) and account for losses and dispersion existing in the line. The maximum attenuation of the UWB pulse amplitude is 6.3 times. Note that the signal at the output of the line has additional delay of 550 ps which can be explained by additional adapters and line outputs on the printed circuit necessary for its connection to the measuring channel. Summary results are given in Table II, where V_1 , V_2 ,

TABLE II
EXPERIMENTAL DEPENDENCIES OF THE AMPLITUDES OF THE FIRST THREE PULSES AND THE DIFFERENCE BETWEEN THEIR PEAKS AT THE OUTPUT OF A MEANDER LINE TURN FROM s

$s, \mu\text{m}$	300	250	200	150
V_1, mV	67.1	71.1	74	79
V_2, mV	93.8	89.9	86	84
V_3, mV	87	83	81.5	81
$\Delta\tau_{21}, \text{ps}$	1016	1016	1012	1012
$\Delta\tau_{32}, \text{ps}$	160	160	164	172

TABLE III
SIMULATION DEPENDENCIES OF THE AMPLITUDES OF THE FIRST THREE PULSES AND THE DIFFERENCE BETWEEN THEIR PEAKS AT THE OUTPUT OF A MEANDER LINE TURN FROM s

$s, \mu\text{m}$	300	250	200	150
V_1, mV	102.5	107.87	114.7	122.6
V_2, mV	201.8	201.3	199.8	198.4
V_3, mV	201.3	201.8	202.3	202.7
$\Delta\tau_{21}, \text{ps}$	1015	1007	1003	992
$\Delta\tau_{32}, \text{ps}$	120.4	126.4	129.1	138.2

V_3 – amplitudes of the first, the second, and the third pulses, $\tau_2 - \tau_1$ – the delay difference of the second and the first pulses, and $\tau_3 - \tau_2$ – the third and the second pulses. These values were measured by oscilloscope markers placed at the points of the maximum impulse voltage.

According to Table II, the decrease of s leads to the increase of the amplitude of the first pulse (crosstalk) and the decrease of the amplitude of the second and the third pulses (even and odd modes). This fact proves that it is possible to minimize amplitudes of a signal at the end of a meander line turn by means of the equalization of the first three pulses. We observe a successive approximation to the optimum choice: the amplitude of the output signal was reduced from 93.8 mV down to 84 mV, and the amplitude of the first pulse was reduced only 5 mV. $\Delta\tau$ increased when the coupling between the conductors strengthened as the gap was reduced, i.e., the signal was decomposed into modes. Thus, the experiment proved the possibility of the decomposition of UWB pulses in the meander microstrip line turn and the possibility of the equalization of amplitudes of the first three pulses at the output of the line, obtained by the optimization of the coupling between signal conductors.

B. Results of the Simulation

In order to compare the results of the full-scale experiment with the results of the simulation, we carried out simulation of the waveform at the end of a turn of a meander line, with excitation taken from Fig. 7 and took into account losses in the conductors and dielectric. Obtained waveforms at the end of models of a meander line are given in Fig. 9, Table III depicts summary results. Matrices of the per-unit-length resistance (\mathbf{R}) and conductivity (\mathbf{G}) were computed to account for losses. Entries of the matrix \mathbf{R} were calculated accounting to the skin effect, but without consideration of the proximity effect. Entries of the matrix \mathbf{G} were computed by means of the well-known

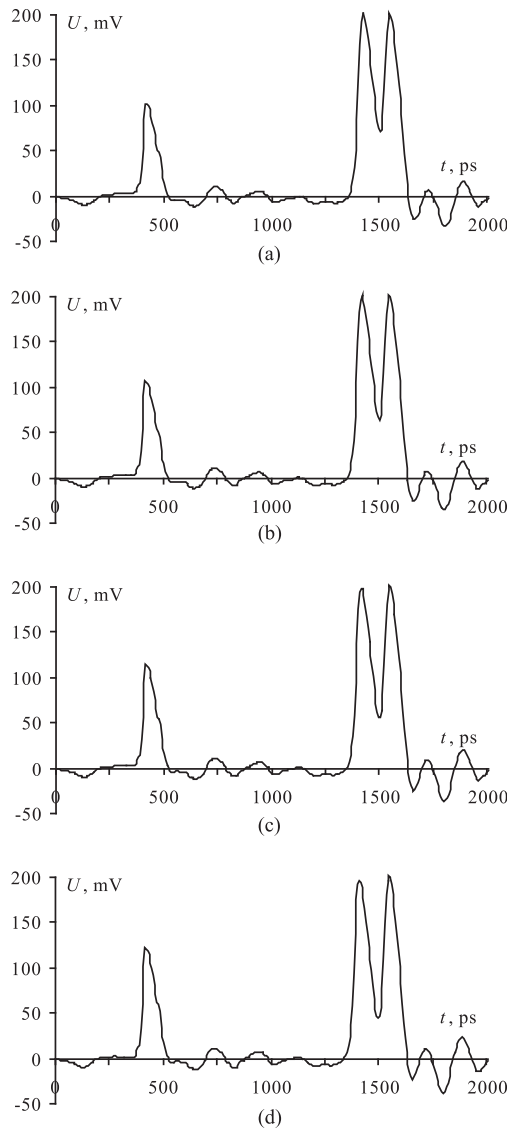


Fig. 9. Waveforms at the output of models of meander lines for $s = 300$ (a), 250 (b), 200 (c), 150 (d) μm .

model of the frequency dependence of relative dielectric permittivity and dielectric loss tangent of the material FR-4 [13]. Matrixes \mathbf{R} and \mathbf{G} at frequency of 1 GHz are equal to

$$\mathbf{R} = \begin{bmatrix} 3.49 & 0 \\ 0 & 3.49 \end{bmatrix} \Omega/\text{m}, \mathbf{G} = \begin{bmatrix} 10.48 & -3.93 \\ -3.93 & 10.48 \end{bmatrix} \text{mSm}/\text{m}.$$

Comparative analysis of Figs. 8 and 9 and Tables II and III shows that the results of the simulation and full-scale experiment have a proper time matching: delay differences of the pulse propagation of the first and the second pulses almost match, experimental values are 1.2–1.3 times higher than simulation ones. At the same time, amplitudes of the signal at the output of meander lines are different. This observation can be explained by the influence of inhomogeneities in connectors and half-turns joint, which were not taken into account in the simulation, the insufficient accuracy of measurements of real parameters of the printed circuit could cause mismatch as well. The amplitude

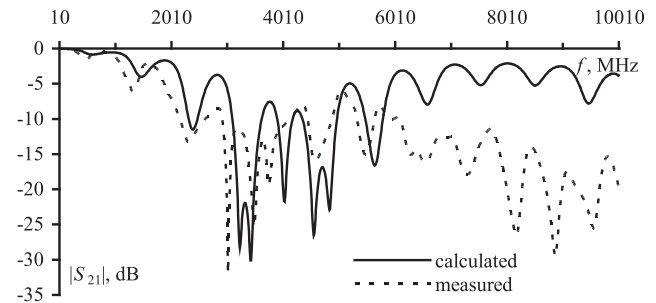


Fig. 10. Calculated (—) and measured (---) frequency dependences of $|S_{21}|$ for meander line turn with $s = 300 \mu\text{m}$.

of the first pulse derived during the simulation is 1.5 times higher than the amplitude derived during the experiment, while amplitudes of the second and the third pulses are 2.1–2.5 times higher. It also proves stronger impact of losses in the real line than in the simulation. In quasistatic simulation, the radiated losses which may influence the coincidence of experiment and simulation results are not taken into account.

C. Discussion

Relying on the results of the real experiment and quasistatic simulation, we can note the positive effect of the proposed approach. Devices can be protected against UWB pulses by the simplest elements of printed circuits – meander lines that decompose UWB pulses into a sequence of pulses. In practice, it is hard to implement this approach for protection of every circuit of a printed circuit assembly. It is easier to implement devices based on meander lines in the most critical and sensitive circuits. As the second option, the proposed approach can be used together with traditional shielding (closure of protected devices in shielded blocks and enclosures). In this case, protective devices based on meander lines with the optimal parameters can be used as intermediate devices between external lines and shielded enclosures; therefore, these devices will provide additional protection against UWB pulses penetrating into blocks via supply circuits.

In general, there are various wanted signals for which various distortions are acceptable. To clarify this issue a frequency response can be useful. We have calculated and measured the frequency dependence of $|S_{21}|$ up to 10 GHz for each of the considered meander line turns. For example, the frequency dependence of $|S_{21}|$ for meander line turn with $s = 0.3 \text{ mm}$ is shown in Fig. 10. One can see that passband of the device is about 1 GHz, warranting the low distortions of wanted signals in this band. Increased discrepancy at higher frequencies can be explained by factors (discontinuities, radiation, and others) not properly considered in simulation.

In practice, the duration and the rise time of a UWB pulse can vary in a wide range of values. Therefore, one turn of a meander line cannot protect against any UWB pulse, but meander line turns can be cascaded to additionally attenuate shorter pulses. The duration of UWB pulses has a very wide range as it does not have a lower range limit and its upper range is limited only by the condition (3). We describe below how to increase the upper range.

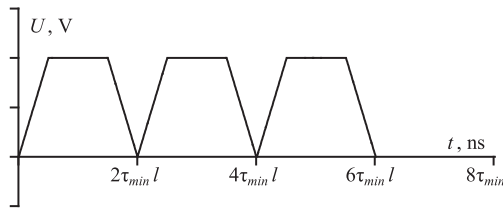


Fig. 11. First three pulses at the end of the turn of a meander line under the condition (5).

By means of the optimization of parameters of the cross section of a meander line, we can obtain the optimum decomposition of a UWB pulse when the second and the third pulses come to the end of the line right after the crosstalk pulse. The condition for such decomposition can be obtained through conditions (2) and (3). Since their right parts are equal, we equalize left parts and replace $|\tau_e - \tau_o|$ with $\tau_{\max} - \tau_{\min}$ (τ_{\max} – the maximum value of per-unit-length delays of even and odd modes of the line) and get

$$2 \cdot (\tau_{\max} - \tau_{\min}) \cdot l = 2 \cdot \tau_{\min} \cdot l. \quad (4)$$

After transformation (4) yields

$$\tau_{\max} = 2 \cdot \tau_{\min}. \quad (5)$$

If the condition (5) is fulfilled due to the optimization of the cross section of the line, three pulses will successively come to the end of the line (see Fig. 11): first, the crosstalk pulse, then pulses of even and odd modes, and each pulse will come to the end of the line right after the previous one. The fulfilled condition (5) increases the duration of a UWB pulse that should be decomposed. The first three pulses will be spread out over a period of time equal to the doubled product of the length of the line and the minimum value of the per-unit-length delay of even and odd modes.

V. CONCLUSION

The paper experimentally proves that the decomposition of a UWB pulse into a sequence of pulses with lower amplitudes in the turn of a meander delay line is an effective method of protection against UWB pulses for electronic equipment. It has been shown that a pulse at the output of a line can be minimized due to the equalization of amplitudes of the first three pulses by means of the optimization of the coupling between half-turns of a line. For this purpose, we optimized parameters of the cross section of models of meander lines, made a printed circuit, and measured its geometric parameters obtained after the printed circuit had been manufactured. A full-scale experiment showed that the maximum attenuation of a UWB pulse amplitude is 6.3 times. We have also carried out the simulation of the experiment (a waveform of a real UWB pulse obtained from the output of a generator during the experiment was taken as excitation, measured parameters of cross section of every line were also taken into account) and compared the obtained results with the results of a full-scale experiment. The comparison proved that the results show a good convergence in propagation delays of the signal components at the output of the line, but we observed a

significant mismatch in pulse amplitudes and explained the reasons for the mismatch. Additionally, calculated and measured frequency dependences are presented. At last, we formulated a condition which provides for pulses successively coming to the end of the line: first, the crosstalk pulse, then pulses of even and odd modes, while each pulse comes to the end of the line right after the previous one.

ACKNOWLEDGMENT

Authors thank reviewers for valuable comments having permitted to improve considerably the paper.

REFERENCES

- [1] Z. M. Gizatullin and R. M. Gizatullin, "Investigation of the immunity of computer equipment to the power-line electromagnetic interference," *J. Commun. Technol. Electron.*, vol. 61, no. 5, pp. 546–550, 2016.
- [2] O. Pektau, A. Tarabartsev, A. Deryabtsev, S. Larionov, and V. Chvanov, "Protection of the fuel & energy sector of threats of electromagnetic influence," *The security and safety of fuel and energy complex facilities*, vol. 6, no. 2, pp. 74–76, 2014 (in Russian).
- [3] Y. Shlepnev, A. Neves, T. Dogostino, and S. McMorro, "Measurement-assisted electromagnetic extraction of interconnect parameters on low-cost FR-4 boards for 6-20 Gb/sec applications," in *Proc. DesignCon 2009*, Feb. 2009, pp. 1–28.
- [4] E. M. T. Jones and J. T. Bolljahn, "Coupled-strip-transmission-line and directional couplers," *IRE Trans. Microw. Theory Tech.*, vol. 4, pp. 75–81, Apr. 1956.
- [5] R. S. Surovtsev, T. R. Gazizov, and A. M. Zabolotsky, "Pulse decomposition in a turn of meander line as a new concept of protection against UWB pulses," in *Proc. Siberian Conf. Control Commun.*, 2015, pp. 1–7.
- [6] R. S. Surovtsev, A. V. Nosov, and A. M. Zabolotsky, "Simple method of protection against UWB pulses based on a turn of meander microstrip line," in *Proc. 16th Int. Conf. Young Spec. Micro/Nanotechnol. Electron Devices EDM 2015*, Jun./Jul. 2015, pp. 175–177.
- [7] A. T. Gazizov, A. M. Zabolotsky, and O. A. Gazizova, "Printed structures for protection against UWB pulses," in *Proc. 16th Int. Conf. Young Spec. Micro/Nanotechnol. Electron Devices EDM 2015*, Jun./Jul. 2015, pp. 120–122.
- [8] A. T. Gazizov, A. M. Zabolotsky, and T. R. Gazizov, "UWB pulse decomposition in simple printed structures," *IEEE Trans. Electromagn. Compat.*, vol. 58, no. 4, pp. 1136–1142, Aug. 2016.
- [9] R. S. Surovtsev, A. M. Zabolotsky, T. R. Gazizov, and P. E. Orlov, "Pulse signal propagation in the meander line with nonhomogeneous dielectric filling without distortions of its waveform by crosstalk," *Dokladi TUSUR*, vol. 4, no. 34, pp. 34–38, Dec. 2014 (in Russian).
- [10] R. S. Surovtsev, T. R. Gazizov, A. V. Nosov, A. M. Zabolotsky, and S. P. Kuksenko, "Meander micro-strip delay line, protecting against ultrashort pulses," Patent RF, No. 2607252, Jan. 10, 2017.
- [11] T. R. Gazizov, "Calculation of a capacitance matrix for a two-dimensional configuration of conductors and dielectrics with orthogonal boundaries," *Russian Phys. J.*, vol. 47, pp. 326–328, 2004.
- [12] S. P. Kuksenko *et al.*, "New developments for improved simulation of interconnects based on method of moments," in *Proc. 2015 Int. Conf. Model. Simul. Appl. Math. Adv. Intell. Syst. Res.*, Aug. 2015, pp. 293–301.
- [13] A. R. Djordjević, R. M. Biljic, V. D. Likar-Smiljanic, and T. K. Sarkar, "Wideband frequency-domain characterization of FR-4 and time-domain causality," *IEEE Trans. Electromagn. Compat.*, vol. 43, no. 4, pp. 662–666, Nov. 2001.



Roman Sergeevich Surovtsev received the Engineering and Ph.D. degrees in engineering science from the Tomsk State University of Control Systems and Radioelectronics (TUSUR), Tomsk, Russia, in 2013 and 2016, respectively.

He is currently a Junior Research Fellow with TUSUR. He is the Author or Coauthor of 60 scientific papers, including 1 book.



Alexander Vyacheslavovich Nosov received the B.E. degree in engineering science from the Tomsk State University of Control Systems and Radioelectronics (TUSUR), Tomsk, Russia in 2015, where he is currently working toward the Master's degree.

He is working as an Engineer with the TUSUR University. He is the Author and Coauthor of 15 scientific papers.



Talgat Rashitovich Gazizov was born in 1963. He received the Engineering, Ph.D., and D.Sc. degrees in engineering science from the Tomsk State University of Control Systems and Radioelectronics, Tomsk, Russia, in 1985, 1999, and 2010, respectively.

He is the Author or Coauthor of 283 scientific papers, including 11 books. His current research interest focuses on signal integrity problem.



Alexander Mikhailovich Zabolotsky received the Engineering and Ph.D. degrees in engineering science from the Tomsk State University of Control Systems and Radioelectronics (TUSUR), Tomsk, Russia, in 2004 and 2010, respectively.

He is currently a Senior Research Fellow with TUSUR. He is the Author or Coauthor of 172 scientific papers, including 7 books.